FEBS Letters 584 (2010) 1609–1614

journal homepage: www.FEBSLetters.org

Site-directed mutagenesis and structural modeling of Coq10p indicate the presence of a tunnel for coenzyme Q6 binding

Cleverson Busso [a], Lucas Bleicher [b], José Ribamar Ferreira-Júnior [c], Mario H. Barros [a,*]

[a] Departamento de Microbiologia, Instituto de Ciências Biomédicas, Universidade de São Paulo, São Paulo, Brazil
[b] Instituto de Física de São Carlos, Universidade de São Paulo, São Carlos, Brazil
[c] Escola de Artes, Ciências e Humanidades, Universidade de São Paulo, São Paulo, Brazil

ARTICLE INFO

Article history:
Received 10 February 2010
Revised 8 March 2010
Accepted 15 March 2010
Available online 18 March 2010

Edited by Vladimir Skulachev

Keywords:
Coenzyme Q
Mitochondrion
COQ10

ABSTRACT

Coq10p is a protein required for coenzyme Q function, but its specific role is still unknown. It is a member of the START domain superfamily that contains a hydrophobic tunnel implicated in the binding of lipophilic molecules. We used site-directed mutagenesis, statistical coupling analysis and molecular modeling to probe structural determinants in the Coq10p putative tunnel. Four point mutations were generated (*coq10-K50E*, *coq10-L96S*, *coq10-E105K* and *coq10-K162D*) and their biochemical properties analysed, as well as structural consequences. Our results show that all mutations impaired Coq10p function and together with molecular modeling indicate an important role for the Coq10p putative tunnel.

1. Introduction

COQ10 encodes a 24 kDa hydrophobic protein necessary for coenzyme Q6 (CoQ6) function in the electron transport chain of mitochondria [1]. Coq10p is a member of the Pfam polyketide cyclase/dehydrase family (PF03364), which includes proteins involved in binding/transport of lipids [2]. It is widely distributed indicating a conserved function. Indeed, the human *COQ10* gene is able to complement *coq10* yeast mutants [1].

In eukaryotes biosynthesis of CoQ occurs in mitochondria, and ten nuclear genes (*COQ1–10*) have been inferred to participate in the synthesis of CoQ6 in *Saccharomyces cerevisiae* [3,4]. Mutants for *COQ1–9* lack CoQ6, but cells depleted of Coq10p have nearly wild type amounts of the coenzyme [1,3]. Nevertheless, in *coq10* mutants NADH and succinate oxidase activities are reconstituted by the addition of synthetic CoQ2 – a hallmark of yeast mutants blocked in CoQ6 respiration [4,5]. Moreover, *coq10* mutants can have their respiratory growth rescued by the over expression of *COQ2*, *COQ7* and *COQ8* [1]. Curiously, *coq10* mutants over expressing *COQ8* have a significant increase in the mitochondrial concentration of CoQ6 [1]. Finally, purified Coq10p from *S. cerevisiae* and *Schizosaccharomyces pombe* were shown to bind to CoQ6 [1,6].

In agreement with these experimental observations, a Coq10p homologue, CC1736 from *Caulobacter crescentus*, was described as a member of the PF03364 family [2,7]. CC1736 does not show sequence similarity to members of the START (StAR-related lipid-transfer) domain superfamily, that are proteins containing a lipid binding domain [8]. However, fold recognition algorithms can recognize their close similarity, which was also confirmed its nuclear magnetic resonance structure. Indeed, structural analysis of *C. crescentus* CC1736 revealed amino acid residues that are crucial for the formation of a hydrophobic tunnel that is putatively required for binding of lipid compounds [7]. Because of Coq10p similarity to CC1736, we used site-directed mutagenesis, statistical coupling ($\Delta\Delta G^{stat}$) analysis and molecular modeling to identify structural determinants in the Coq10p putative hydrophobic tunnel. Our data support the hypothesis that Coq10p has a tunnel structure similar to that of CC1736, which is necessary to Coq10p function and may be required for CoQ6 binding.

2. Materials and methods

2.1. Yeast strains and media

The yeast strains used in this study were W303-1A (*MAT*a, ρ^+, *ade2-1 can1-100 his3-11, 15 leu2-3, 112 trp1-1 ura3-1*) and a *coq10Δ*

Abbreviations: CoQ, coenzyme Q; NMR, nuclear magnetic resonance; RMSD, root mean square deviation; $\Delta\Delta G^{stat}$, statistical coupling

* Correspondence to: Mario H. Barros, Departamento de Microbiologia, ICB-II, Universidade de São Paulo, Av. Prof. Lineu Prestes, 1374, Cidade Universitária, 05508-900 São Paulo, SP, Brazil. Fax: +55 11 30917354.
E-mail address: mariohb@usp.br (M.H. Barros).

0014-5793/$36.00
doi:10.1016/j.febslet.2010.03.024

isogenic derivative [1]. Composition of growth media have been described elsewhere [1].

2.2. Construction of coq10 point mutant alleles

coq10-K50E, *coq10-L96S*, *coq10-E105K* and *coq10-K162D* mutants alleles were obtained after two independent PCR reactions of the wild type *COQ10*. In each case, a restriction site was created by silent mutagenesis near the desired mutated position in order to facilitate the cloning. The alleles were cloned in either YIp351 or YIp352, and then transferred to YEp352 [9].

2.3. NADH-cytochrome c activity determination, O_2 consumption and H_2O_2 release measurements

NADH-cytochrome *c* reductase activity was assayed at 23 °C from isolated mitochondria as previously described [5]. Mitochondria were prepared from yeast grown in rich media containing galactose as a carbon source [10]. Briefly yeast cells were incubated in the presence of Zymolyase 20 000 (1 mg/ml) (ICN, CA) and spheroplasts resuspended in 10 ml/g of lysis buffer (0.6 M Sorbitol 10 mM Tris–Cl [pH 7.5], 1 mM EDTA) and then gently broken in a glass homogenizer. Intact cells and cell debris were removed by centrifugation at 1000×*g* for 10 min. The supernatant was centrifuged at 17 000×*g* for 10 min, and then the pellet washed four more times at the same conditions in order to maximize the presence of intact mitochondria.

O_2 consumption of yeast spheroplasts was monitored over time at 30 °C, in the presence of 2% ethanol and 1 mM malate/glutamate, using a computer-interfaced Clark-type electrode. To distinguish respiration from cyanide-insensitive O_2 consumption, 1 mM KCN was added.

Measurements of H_2O_2 release also employed spheroplasts that were incubated with 0.5 U/ml horseradish peroxidase and 50 μM Amplex Red. Samples were excited at 563 nm and the fluorescence of oxidized Amplex Red (resorufin) measured at 587 nm.

2.4. Statistical coupling analysis

Coq10p homologue protein sequences were obtained from the non-redundant database by using PSI-BLAST [11]. This allowed the retrieval of 491 unique sequences that were aligned in the program Clustal W [12]. This multiple sequence alignment was used for the calculation of positional conservation and $\Delta\Delta G^{stat}$ [13,14].

2.5. Model building

Three dimensional models were built using homology modeling as implemented in Geno3D [15] and threading as in I-Tasser [16]. For the homology model, the structure of CC1736 from *C. crescentus*

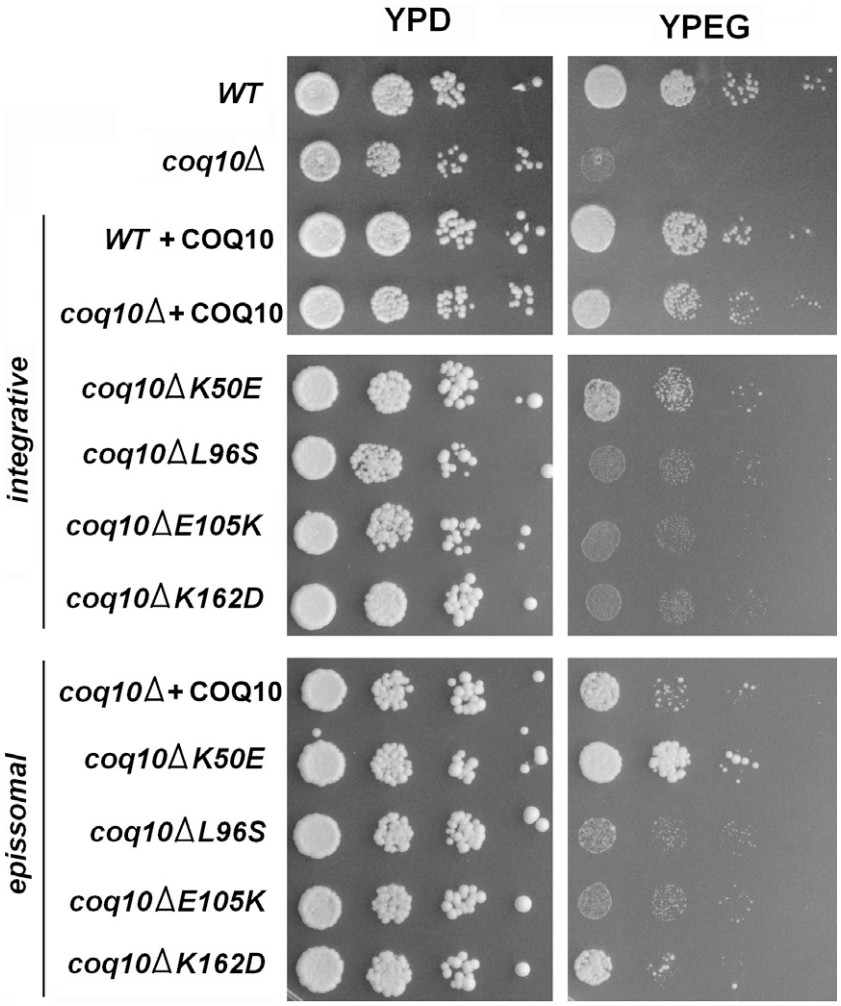

Fig. 1. Growth properties of *coq10* point mutants. Wild type (WT), *coq10Δ*, and *coq10Δ* cells were transformed with either integrative or episomal plasmids, containing different *coq10* mutant alleles (K50E, L96S, E105K and K162D) and the *COQ10* wild type allele. Cells were spotted on rich glucose (YPD) and rich ethanol/glycerol (YPEG) plates and incubated at 30 °C for 48 h.

Table 1
NADH-cytochrome *c* reductase activity.[a]

Strain[b]	ρ⁺ (%)	CoQ2 (μM)			
		0	0.12	1.2	4
W303-1A	98	1.3 ± 0.08	1.42 ± 0.05	1.43 ± 0.02	1.69 ± 0.09
coq10Δ	65	0.24 ± 0.04	0.33 ± 0.02	0.63 ± 0.1	1.0 ± 0.02
coq10-K50E	65	0.34 ± 0.01	0.68 ± 0.01	0.92 ± 0.02	0.93 ± 0.09
coq10-L96S	85	0.46 ± 0.02	0.54 ± 0.01	0.85 ± 0.05	1.2 ± 0.01
coq10-E105K	80	0.36 ± 0.03	0.51 ± 0.02	0.92 ± 0.05	1.12 ± 0.01
coq10-K162D	90	0.61 ± 0.01	0.67 ± 0.01	1.08 ± 0.02	1.27 ± 0.02

[a] Activity is measured in μmoles cytochrome *c* reduced/min/mg protein. Values reported are average of two independent assays expressed as mean ± S.D.
[b] *coq10* mutant alleles were integrated into the genome of *coq10Δ* strain.

was used as a template [7]. Root mean square deviation for Cα–Cα superposition between the two models was 1.58 Å. Figures were generated using PyMOL [17].

3. Results

3.1. Coq10p putative tunnel amino acids are essential for respiratory growth

The *C. crescentus* CC1736 protein is a member of the START domain super family that contains a hydrophobic tunnel involved in biding/transport of lipids [7,8,18]. Four amino acid residues of CC1736 were previously identified as important for tunnel formation and ligand binding [7]. Because Coq10p is a CC1736 homologue, we used PCR site-directed mutagenesis to create the mutations K50E, L96S, E105K and K162D, which lie inside Coq10p putative hydrophobic tunnel. These mutants were transformed into *coq10Δ* yeast and their ability to grow in respiratory medium (YPEG) analyzed. When expressed in single copy (integrative), all new *coq10* alleles showed impairment in their respiratory growth (Fig. 1). However, when *coq10* alleles K50E and K162D are expressed in multi-copy (episomal) plasmids, an improvement of respiratory growth was clearly detected. This growth rescue suggests that the partial loss of function in K50E and K162D can be suppressed by over-expressing these alleles. Altogether, these phenotypes indicate that mitochondrial respiration is reduced when *coq10* mutants are expressed in *coq10Δ* background.

3.2. Respiratory efficiency of the coq10 mutants

To further investigate the effect of *coq10* alleles on mitochondrial respiration we analyzed NADH-cytochrome *c* reductase activity in isolated mitochondria, oxygen consumption and H_2O_2 release in spheroplasts. All the mutant strains are NADH-cytochrome *c* reductase deficient when compared to wild type (Table 1), and their activities could be restored upon addition of synthetic CoQ2. However, without CoQ2 additions, oxygen consumption measurements showed a lower respiratory rate for all *coq10* alleles (Fig. 2A), which was accompanied by an increase in reactive oxygen species (ROS), as observed by H_2O_2 measurements (Fig. 2B). H_2O_2 release is an indicative of leakage of electrons emanating from NADH and succinate reduce oxygen to the superoxide anion O_2^-, which can be estimated by measuring its dismutation to H_2O_2 [19]. Interruption of the electron transport chain at the *bc*1 complex level enhances significantly electron leakage and consequently raises the level of H_2O_2 [20]. Taken together with the polarographic studies and NADH-cytochrome *c* reductase activity, these data indicate that *coq10* putative tunnel mutants and the *coq10* null mutant have similar respiratory efficiency.

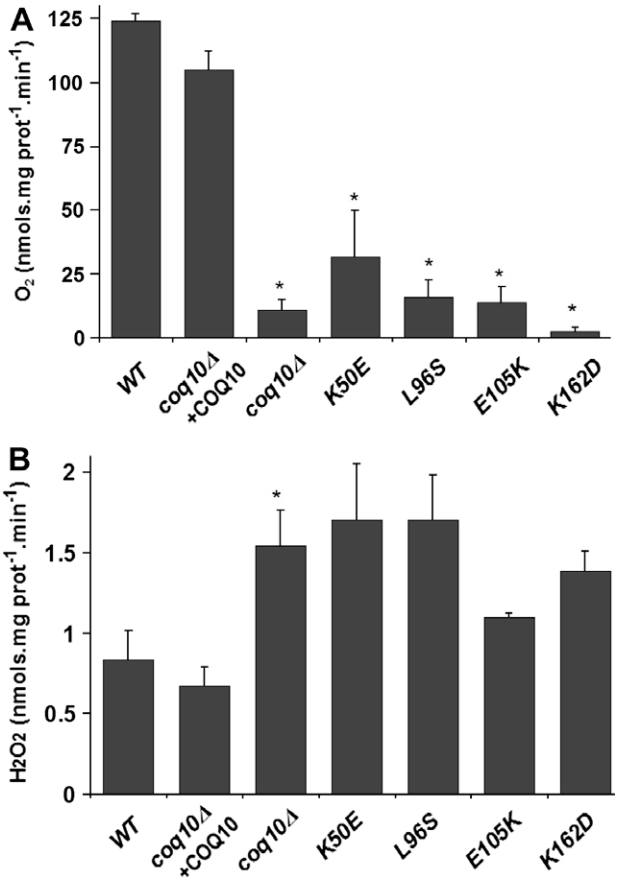

Fig. 2. Respiratory activity and hydrogen peroxide release of *coq10* mutant strains. Oxygen consumption (A) and H_2O_2 release (B) were measured in spheroplasts for the strains wild type (WT), *coq10Δ*, and *coq10Δ* transformed with the integrative mutant alleles K50E, L96S, E105K and K162D and the *COQ10* wild type allele. Values are average of three independent experiments with similar results. *$P < 0.05$% versus WT.

3.3. Statistical coupling analysis

The ClustalW alignment of 491 Coq10p homologue sequences revealed that selected positions K50, L96, E105 and K162 are all moderately conserved (Fig. 3A). Position 50 shows a preference for residues with either positive (arginine and lysine) or polar (glutamine) character; position 96 is widely dominated by leucines and methionines; position 105 shows an acidic residue (glutamic acid) in half of the sequences, but also presents lysines and glutamines at lower frequencies. Finally, position 162 can either have a polar (serine) or a positive residue (lysine or arginine). Given these amino acid distributions we observed that mutations K50E, L96S and K162D are clearly against the overall trend in amino acid conservation for their respective positions, which is consistent with the growth impairment observed (Fig. 1). The position 105, however, needs to be analyzed in detail, because the moderately conserved mutation E105K would still be compatible with the overall trend.

Moderately conserved positions are suitable targets for $\Delta\Delta G^{stat}$ analysis [21]. Partial conservation could mean that (1) two or a few possible amino acids are compatible with a given functional or structural feature of that position, independently of what is present in the rest of the protein, or (2) the amino acids options allowed in that specific position are dependent on one or more positions in other sites of the protein. To determine which is the case one should measure the $\Delta\Delta G^{stat}$ between all other positions

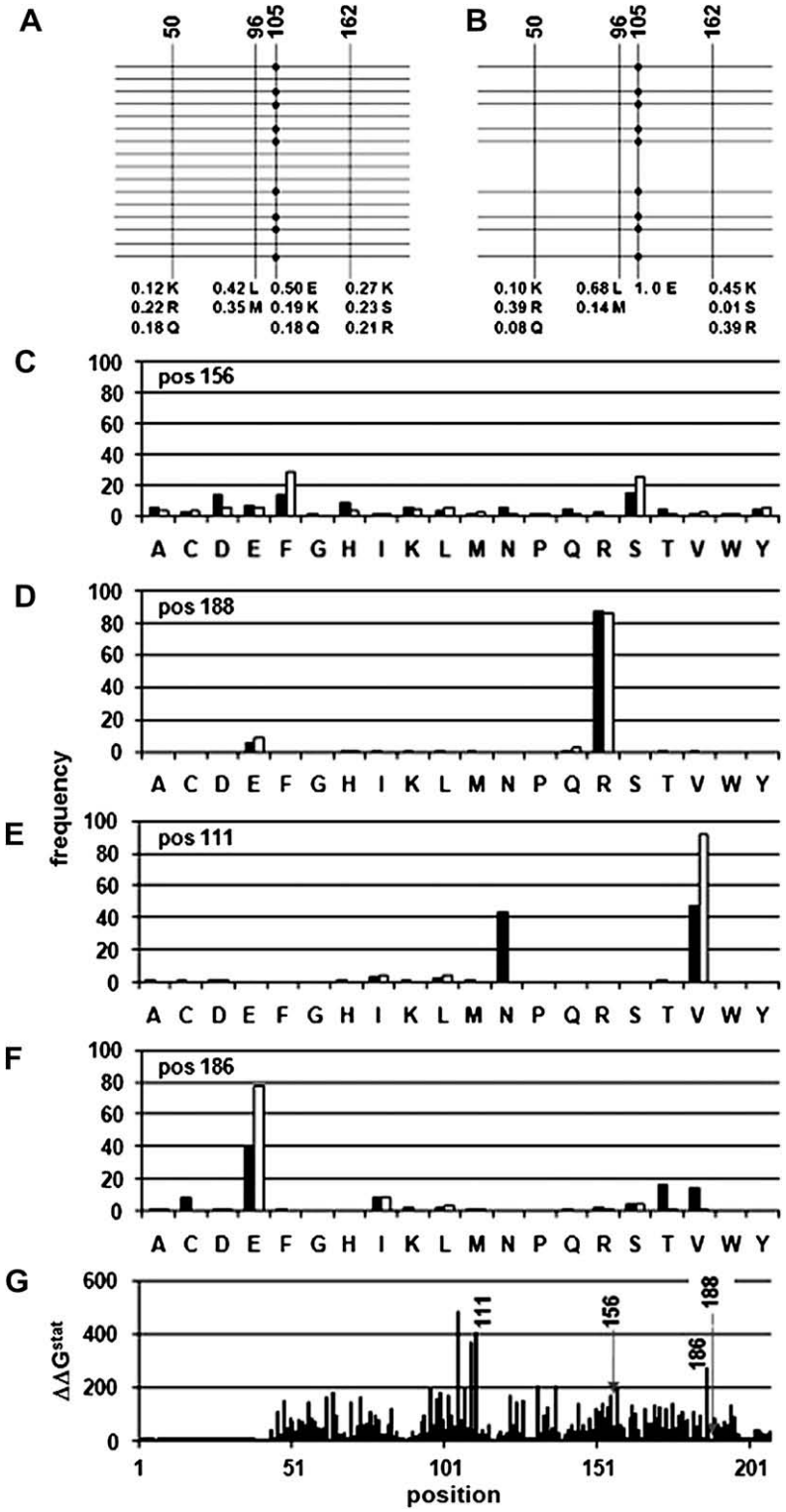

Fig. 3. Statistical coupling analysis of *Coq10p*. (A) Schematic representation of the alignment showing the mutated sites and their frequency distributions for dominant amino acids. Residue number is based in *S. cerevisiae* Coq10p primary sequence. (B) Subalignment containing 242 sequences after E105 perturbation. (C–F) Amino acid frequency distribution at the indicated position: full alignment (black bars), subalignment (white bars). (C) Position 156 is neither conserved nor coupled. (D) Position 188 is conserved but not coupled. (E) Position 111 and (F) position 186 are conserved and coupled to E105. (G) Complete statistical coupling for all amino acid positions calculated for the E105 perturbation.

in the protein and the given site. High values of $\Delta\Delta G^{stat}$ would mean that the choice is dependent on those positions, whereas low values indicate that the amino acid option is not influenced by the existence of other amino acids in the protein. In other words, by extracting a subset of the 491 sequence alignment in which only glutamate is present in position 105, one can determine the distribution of all the other amino acids and look for those residues whose frequency also increases (Fig. 3C–G).

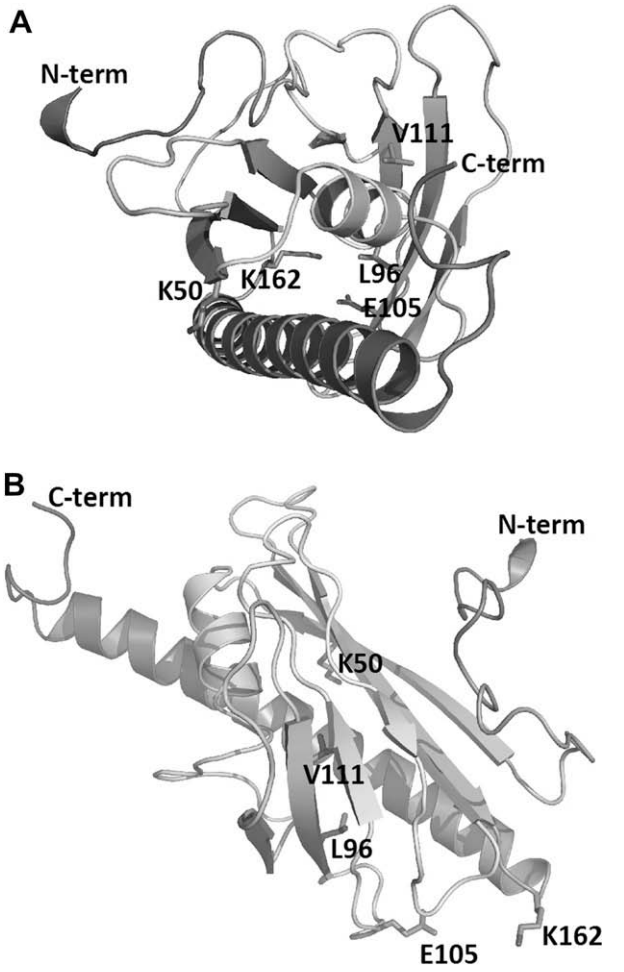

Fig. 4. *Coq10p* modeled structure: top (A) and side (B) views of Coq10p model and threading as implemented using the three-dimensional model generated by I-Tasser. The positions of mutated residues are indicated in the figure, which was rendered in PyMol.

By imposing glutamate at position 105 we obtained a subalignment with 242 sequences (Fig. 3B) that was used for determining the $\Delta\Delta G^{stat}$ (Fig. 3G). This perturbation showed not to be significant for position 156, which is unconserved in the subalignment (Fig. 3C). Conversely, although position 188 is conserved before and after the perturbation, its frequency neither increases nor decreases, and therefore is not coupled (Fig. 3D). However, positions 111 and 186 have their amino acid frequencies dramatically increased for valine and glutamic acid, respectively, indicating strong coupling between position 105 and these sites (Fig. 3E and F). Moreover, all the other Coq10p mutated sites are not substantially affected in their amino acids distributions by the perturbation E105 (compare Fig. 3A and B). Taken together these data show that selected mutated residues are either strongly conserved or coupled and this may explain their relevance observed in both growth phenotype and biochemical data.

3.4. Coq10p modeling

Models for Coq10p were subjected to structural alignment to the known START domains of CC1736 from *C. crescentus* (PDB code: 1T17), StarD4 from *Mus musculus* (PDB code: 1JSS), the human StAR-related lipid transport domain from MLN64 (PDB code: 1EM2) and the polyketide cyclase SnoaL from *Streptomyces nogalater* (PDB code: 1SJW). All of them share the same fold aspect, with a tunnel formed mostly by beta-sheets, with a high variety of sequences and features in the tunnel (Fig. 4A).

The START domain in StartD4 from *M. musculus* possesses a charged pair lying in the interior of the tunnel, proposed to be important for cholesterol specificity [18]. On the other hand, CC1736 from *C. crescentus*, has this pair substituted by two hydrophobic residues, suggesting different ligand specificities in the tunnel. Coq10p also has a hydrophobic pair, composed of V111 and L96. Changing the hydrophobic character of position 96, as seen in the L96S mutation, has a deleterious result (Fig. 1). Furthermore, CC1736 has a salt bridge, formed by E64 and K115, which lies at the entrance of the tunnel, and it is suggested to determine ligand specificity [7]. In Coq10p, the equivalent residues are E105 and K162, which probably also form a salt bridge as seen in the models (Fig. 4B). Therefore E105K and K162D mutations would disrupt this salt bridge. Finally, residue K8 in CC1736 that is responsible for the positive electrostatic potential at one end of the tunnel, has K50 as a counterpart in Coq10p (Fig. 4A), and changing its character in the mutation K50E resulted in the mildest respiratory growth defect, among the selected mutants (Fig. 1).

4. Discussion

Previous works showed that Coq10p may directly bind to CoQ6 [1,6] but there are no three-dimensional structural studies regarding to the determinants for this binding. In order to probe these determinants, we generated a multiple sequence alignment of Coq10p homologues and selected four conserved residues for site-directed mutagenesis. These residues lie at the putative hydrophobic tunnel formed by the START domain of the protein, as indicated by structural modeling (Fig. 4). This domain is known to bind lipophilic molecules such as cholesterol and polyketides [8].

StAR (steroidogenic acute regulatory protein) is a mitochondrial protein representative of the START family well known to act as cholesterol transporter [21]. CoQ6 is also a lipophilic molecule and we propose here that CoQ6 should be a substrate of Coq10p putative tunnel, which would be necessary for the protein function. Indeed, mutant alleles that disturb this putative tunnel result in respiratory deficient strains (Fig. 2A). The *coq10* point mutants also share relevant biochemical properties with the coq10 null mutant. For instance, exogenous CoQ2 restores NADH-cytochrome *c* reductase activity in the *coq10* mutants (Table 1), as well as in the *coq1–9* mutants [1,3–5]. Even though *coq10* null mutant have wild type amounts of CoQ6 [1], its respiration and NADH and succinate oxidation can be rescued by the addition of CoQ2, a compound more soluble than CoQ6. In addition, H_2O_2 release is higher in these mutants when compared to wild type indicating an increment of electrons leakage from the respiratory chain.

Cui and Kawamukai [6] mutated 13 highly conserved hydrophobic residues in *S. pombe* Coq10p homologue (SpCoq10p), and found that L63A and W104A mutations result in defective respiration and growth retardation in minimal medium. Moreover, both single mutants and the double mutant L63A/W104A showed lower CoQ-binding activity. We also modeled the structure of SpCoq10p (data not shown) and verified that these residues lie inside the putative tunnel of the protein. This supports our hypothesis and indicates that tunnel residues may be required to CoQ6 binding.

Finally, $\Delta\Delta G^{stat}$ analysis showed that the residues E105 and V111 are coupled. This means that for most Coq10p homologues, E105 and V111 should be present simultaneously, suggesting a functional role for those residues, which according to our model are inside the tunnel. This suggests that coevolution of these residues was directed by the protein function that requires the inside of the START domain.

The specific function of Coq10p is still unveiled; one possible function would involve the CoQ6 transport by Coq10p from its site of synthesis to its proper location for electron transport. Here we show the properties of the START domain of Coq10p and its probable involvement in the binding of CoQ6 [1,6].

Acknowledgements

We are indebted to Alicia J. Kowaltowski and Erich B. Tahara (IQ-USP). This work was supported by CNPq and FAPESP.

References

[1] Barros, M.H., Johnson, A., Gin, P., Marbois, B.N., Clarke, C.F. and Tzagoloff, A. (2005) The *Saccharomyces cerevisiae* COQ10 gene encodes a START domain protein required for function of coenzyme Q in respiration. J. Biol. Chem. 280, 42627–42635.

[2] Bateman, A., Birney, E., Cerruti, L., Durbin, R., Etwiller, L., Eddy, S.R., Griffiths-Jones, S., Howe, K.L., Marshall, M. and Sonnhammer, E.L. (2002) The Pfam protein families database. Nucleic Acids Res. 30, 276–280.

[3] Tran, U.C. and Clarke, C.F. (2007) Endogenous synthesis of coenzyme Q in eukaryotes. Mitochondrion 7 (Suppl. 1), S62–S71.

[4] Tzagoloff, A. and Dieckmann, C.L. (1990) PET genes of *Saccharomyces cerevisiae*. Microbiol. Rev. 54, 211–225.

[5] Tzagoloff, A., Akai, A. and Needleman, R.B. (1975) Assembly of the mitochondrial membrane system. Characterization of nuclear mutants of *Saccharomyces cerevisiae* with defects in mitochondrial ATPase and respiratory enzymes. J. Biol. Chem. 250, 8228–8235.

[6] Cui, T.Z. and Kawamukai, M. (2009) Coq10, a mitochondrial coenzyme Q binding protein, is required for proper respiration in *Schizosaccharomyces pombe*. FEBS J. 276, 748–759.

[7] Shen, Y., Goldsmith-Fischman, S., Atreya, H.S., Acton, T., Ma, L., Xiao, R., Honig, B., Montelione, G.T. and Szyperski, T. (2005) NMR structure of the 18 kDa protein CC1736 from *Caulobacter crescentus* identifies a member of the START domain superfamily and suggests residues mediating substrate specificity. Proteins 58, 747–750.

[8] Ponting, C.P. and Aravind, L. (1999) START: a lipid-binding domain in StAR, HD-ZIP and signalling proteins. Trends Biochem. Sci. 24, 130–132.

[9] Hill, J.E., Myers, A.M., Koerner, T.J. and Tzagoloff, A. (1986) Yeast/*E. coli* shuttle vectors with multiple unique restriction sites. Yeast 2, 163–167.

[10] Herrmann, J.M., Foelsch, H., Neupert, W. and Stuart, R.A. (1994) Isolation of yeast mitochondria and study of mitochondrial protein translation (Celis, J.E., Ed.), Cell Biology: A Laboratory Handbook, Vol. I, pp. 538–544, Academic Press, San Diego, CA.

[11] Altschul, S.F., Madden, T.L., Schaffer, A.A., Zhang, J., Zhang, Z., Miller, W. and Lipman, D.J. (1997) Gapped BLAST and PSI-BLAST: a new generation of protein database search programs. Nucleic Acids Res. 25, 3389–3402.

[12] Thompson, J.D., Higgins, D.G. and Gibson, T.J. (1994) CLUSTAL W: improving the sensitivity of progressive multiple sequence alignment through sequence weighting, position-specific gap penalties and weight matrix choice. Nucleic Acids Res. 22, 4673–4680.

[13] Lockless, S.W. and Ranganathan, R. (1999) Evolutionarily conserved pathways of energetic connectivity in protein families. Science 286, 295–299.

[14] Bachega, J.F., Navarro, M.V., Bleicher, L., Bortoleto-Bugs, R.K., Dive, D., Hoffmann, P., Viscogliosi, E. and Garratt, R.C. (2009) Systematic structural studies of iron superoxide dismutases from human parasites and a statistical coupling analysis of metal binding specificity. Proteins 77, 26–37.

[15] Combet, C., Jambon, M., Deleage, G. and Geourjon, C. (2002) Geno3D: automatic comparative molecular modelling of protein. Bioinformatics 18, 213–214.

[16] Zhang, Y. (2008) I-TASSER server for protein 3D structure prediction. BMC Bioinf. 9, 40.

[17] DeLano, W.L. (2002) The PyMol Molecular Graphics System, DeLano Scientific, San Carlos, CA.

[18] Romanowski, M.J., Soccio, R.E., Breslow, J.L. and Burley, S.K. (2002) Crystal structure of the *Mus musculus* cholesterol-regulated START protein 4 (StarD4) containing a StAR-related lipid transfer domain. Proc. Natl. Acad. Sci. USA 99, 6949–6954.

[19] Boveris, A. and Chance, B. (1973) The mitochondrial generation of hydrogen peroxide. General properties and effect of hyperbaric oxygen. Biochem. J. 134, 707–716.

[20] Dröse, S. and Brandt, U. (2008) The mechanism of mitochondrial superoxide production by the cytochrome bc1 complex. J. Biol. Chem. 283, 21649–21654.

[21] Lin, D., Sugawara, T., Strauss 3rd, J.F., Clark, B.J., Stocco, D.M., Saenger, P., Rogol, A. and Miller, W.L. (1995) Role of steroidogenic acute regulatory protein in adrenal and gonadal steroidogenesis. Science 267, 1828–1831.